Neurobiology of Disease 40 (2010) 518–530

Contents lists available at ScienceDirect

Neurobiology of Disease

journal homepage: www.elsevier.com/locate/ynbdi

The dopamine transporter is differentially regulated after dopaminergic lesion

Domingo Afonso-Oramas [a], Ignacio Cruz-Muros [a,d], Pedro Barroso-Chinea [b,d], Diego Álvarez de la Rosa [c], Javier Castro-Hernández [a], Josmar Salas-Hernández [a], Teresa Giráldez [e], Tomás González-Hernández [a,d,*]

[a] Departamento de Anatomía, Facultad de Medicina, Universidad de La Laguna, Tenerife, Spain
[b] Centro de Investigación Médica Aplicada, Universidad de Navarra, Spain
[c] Departamento de Fisiología, Facultad de Medicina, Universidad de La Laguna, Tenerife, Spain
[d] Centro de Investigación Biomédica en Red de Enfermedades Neurodegenerativas, Instituto de Salud Carlos III, Spain
[e] Unidad de Investigación, Hospital Universitario Ntra Sra de Candelaria, Tenerife, Spain

ARTICLE INFO

Article history:
Received 29 April 2010
Revised 9 July 2010
Accepted 22 July 2010
Available online 2 August 2010

Keywords:
Parkinson's disease
Vulnerability
Mesostriatal
Degeneration
Dopamine transporter
Rat
HEK-cell
6-OHDA
MPP^+

ABSTRACT

The dopamine transporter (DAT) is a transmembrane glycoprotein responsible for dopamine (DA) uptake, which has been shown to be involved in DA-cell degeneration in Parkinson's disease (PD). At the same time, some studies suggest that DAT may be regulated in response to dopaminergic injury. We have investigated the mechanisms underlying DAT regulation after different degrees of dopaminergic lesion. DAT is persistently down-regulated in surviving midbrain DA-neurons after substantial (62%) loss of striatal DA-terminals, and transiently after slight (11%) loss of DA-terminals in rats. Transient DAT down-regulation consisted of a decrease of glycosylated (mature) DAT in the plasma membrane with accumulation of non-glycosylated (immature) DAT in the endoplasmic reticulum-Golgi (ERG) compartment, and recovery of the normal expression pattern 5 days after lesion. DAT redistribution to the ERG was also observed in HEK cells expressing rat DAT exposed to MPP^+, but not after exposure to DAT-unrelated neurotoxins. In contrast to other midbrain DA-cells, those in the ventrolateral region of the substantia nigra do not regulate DAT and degenerate shortly after slight DA-lesion. These data suggest that DAT down-regulation is a post-traslational event induced by DA-analogue toxins, consisting of a stop in its glycosylation and trafficking to the plasma membrane. Its persistence after substantial DA-lesion may act as a compensatory mechanism helping maintain striatal DA levels. The fact that neurons which do not regulate DAT die shortly after lesion suggests a relationship between DAT down-regulation and neuroprotection.

Introduction

The dopamine transporter (DAT) is a membrane glycoprotein specific to dopaminergic (DA-) cells, whose physiological role is the reuptake of released dopamine (DA) into presynaptic DA-terminals, regulating the time and intensity of DA signalling in extracellular space (Amara and Kuhar, 1993; Gainetdinov et al., 1998b; Giros and Caron, 1993; Uhl, 2003). Given that the cytosolic levels of DA directly depend on DA uptake, and that DA metabolism is the main source of reactive oxygen species in DA-cells (Adams et al., 2001; Luo and Roth, 2000), DAT has also been involved in the degeneration of DA-cells in Parkinson's disease (PD). This idea is supported by evidence of an anatomical correlation between the distribution of DA-neurons expressing high DAT mRNA levels and those showing high vulnerability to degeneration in PD (Cerruti et al., 1993; Hurd et al., 1994; Uhl et al., 1994), and by the fact that DAT can also transport natural and synthetic DA-analogue neurotoxins (Blum et al., 2001; Schober, 2004). Furthermore, its pharmacological blockade or deficient expression makes DA-cells resistant to these neurotoxins (Bezard et al., 1999; Gainetdinov et al., 1997; Kopin, 1992). The finding of an increase in the relative extracellular concentration of DA after a partial lesion of the mesostriatal system has suggested that DAT may at the same time be regulated in response to a DAergic insult (Bezard et al., 2001; Stachowiak et al., 1987), and consequently during the course of PD. This idea is reinforced by *in vitro* studies reporting a DA uptake decrease in striatal synaptosomes and DAT transfected cells after exposure to oxygen radicals or 1-methyl-4-phenylpyridinium (MPP^+), the active metabolite of the DA-analogue neurotoxin 1-methyl-4-phenyl-1,2,3,6-tetrahydropyridine (MPTP) (Berman et al., 1996; Chagkutip et al., 2003; Fleckenstein et al., 1997a; Gulley et al., 2002). However, important aspects concerning this phenomenon are still unknown. The clarification of details such as the lesion degree required for inducing DAT

Abbreviations: DA, domanine; dSt, dorsal striatum; glyco-DAT, glycosylated DAT form; MPP^+, 1-methyl-4-phenylpyridinium; non-glyco-DAT, non-glcyosylated DAT form; SNcv, substantia nigra, caudoventral and lateral region; SNrm, substantia nigra, rostromedial and dorsal region; vSt, ventral striatum; VTA, ventral tegmental area; 6-OHDA, 6-hydroxydopamine.

* Corresponding author. Department of Anatomy, Faculty of Medicine, University of La Laguna, 38207 La Laguna, Tenerife, Spain. Fax: +34 922 660253.
E-mail address: tgonhern@ull.es (T. González-Hernández).

Available online on ScienceDirect (www.sciencedirect.com).

0969-9961/$ – see front matter © 2010 Elsevier Inc. All rights reserved.
doi:10.1016/j.nbd.2010.07.012

expression changes, if all midbrain DA-cells respond similarly to the neuronal insult, and which cellular mechanisms are involved in this phenomenon, will provide further insight into the role of DAT in the pathogenesis of PD. This study has been focused on these questions by using molecular, morphological and pharmacological techniques in animal and cellular models of PD.

Material and methods

Intracerebroventricular injection of 6-hydroxydopamine in rats

6-hydroxydopamine (6-OHDA) is a hydroxylated analogue of DA which has been used extensively in animal models of PD. Similarly to DA, 6-OHDA has a high affinity for DAT, which carries the toxin inside the DA-neuron. Once inside the cell, 6-OHDA undergoes auto-oxidation producing oxidative stress because of the formation of free radials (Blum et al., 2001; Schober, 2004). We have developed a rat model of PD based on the intracerebroventricular (i.c.v.) injection of 6-OHDA which causes bilateral and dose-dependent degeneration of mesostriatal DA-neurons, and a motor syndrome composed of hypokinesia, purposeless chewing and catalepsy (Gonzalez-Hernandez et al., 2004; Rodriguez et al., 2001a, 2001b). Furthermore, the topographical pattern of DA-cell degeneration matches that observed in PD (Damier et al., 1999; Hirsch et al., 1988). The loss of DA-cells in the caudo-ventral and lateral region of the substantia nigra (SNcv) is higher than that in its rostro-dorsal and medial region (SNrm), and is higher in this region than in the ventral tegmental area (VTA). In order to study the effects of two different degrees of DA-lesion, animals were injected with either 150 μg or 350 μg of 6-OHDA in this work.

Experimental protocols were approved by the Ethical committee of the University of La Laguna (Reference #091), and are in accordance with the European Communities Council Directive of 24 November 1986 (86/609/EEC) regarding the care and use of animals for experimental procedures. Anaesthesia, pre-surgery treatment and intraventricular injection protocols followed Rodriguez et al. (2001a; 2001b). A total of 45 male Sprague–Dawley rats (350–400 g) supplied by Charles River (L'Arbresle, France) were used. They were injected in the third ventricle with vehicle (0.9% saline solution with 0.3 μg/μl ascorbic acid, $n=10$) or a single dose (150 μg, $n=30$, or 350 μg, $n=5$) of 6-OHDA (6-hydroxydopamine hydrochloride, Sigma, St. Louis, MO; in 7.5 μl of vehicle per injection; 1 μl/min). Bearing in mind that the bilateral degeneration of DA-cells can cause adipsia and aphagia (Ungerstedt, 1971; Zigmond and Stricker, 1973), the intake of food and water was monitored following the 6-OHDA injection. No body weight loss was observed. Rats were killed at 24 h, 48 h, 5 days or 3 weeks after injection.

DAT antibodies

DAT expression was studied by immunohistochemistry and western-blot using antibodies raised against different DAT fragments which recognize the glycosylated and non-glycosylated DAT forms. The characterization of these antibodies is described in supplementary material. See also Cruz-Muros et al. (2009).

Morphological study

Animals were deeply anaesthetised (chloral hydrate, 400 mg/kg, ip) and transcardially perfused with 0.9% saline (150 ml) and 4% paraformaldehyde in 0.1 M phosphate-buffered saline pH 7.4 (PBS, 400 ml). Midbrains and forebrains were immersed in a cryoprotective solution of 30% sucrose in the same buffer overnight at 4 °C, cut into 25 μm coronal sections (50 μm thick for cell count) with a freezing microtome, and collected in 6–8 parallel series. Solutions used for perfusion and cryoprotection were treated with 0.1% diethylpyrocarbonate (DEPC) and autoclaved to inactivate RNases.

Immunohistochemistry

Midbrain and forebrain sections were processed for DAT and TH immunohistochemistry according to the procedure previously described (Gonzalez-Hernandez et al., 2004), and using the following primary antibodies: rabbit anti-DAT polyclonal antibody (sc-14002, 1:400, for non-glycosylated DAT labelling), rat anti-DAT monoclonal antibody (MAB369, 1:800; for glycosylated DAT labelling), and mouse anti-TH monoclonal antibody (Sigma, 1:12,000). Immunoreactions were visible after incubation for 1 h at RT in ExtrAvidin-peroxidase (1:5000, Sigma) in PBS, and after 10 min in 0.005% 3'-3'-diamiobenzidine tetrahydrochloride (DAB, Sigma) and 0.001% H_2O_2 in cacodylate buffer 0.05 N pH 7.6.

Fluoro-Jade histofluorescence

Fluoro-Jade staining is a sensitive histofluorescent technique for detecting degenerated neurons in brain tissue (Schmued et al., 1997; Schmued and Hopkins, 2000). This tracer was used to reveal neuronal degeneration 48 h after 6-OHDA injection. Briefly, midbrain sections were mounted with distilled water onto 3-aminopropyltriethoxysilane (APS) coated slides and air-dried at RT for 40 min. The slides were immersed for 3 min in 100% ethyl alcohol, and in 70% alcohol and distilled water for 1 min. They were then transferred to a solution of 0.06% potassium permanganate for 15 min, rinsed for 1 min in distilled water and incubated for 30 min in 0.001% Fluoro-Jade (Histo-Chem, Jefferson, AR) in 0.09% acetic acid. After staining, the sections were rinsed several times in distilled water, dehydrated, immersed in xylene and coverslipped with PDX (BDH Chemicals).

Quantitative analysis of immunostained sections

Bearing in mind the functional division of the mesostriatal system (Fallon and Moore, 1978; Joel and Weiner, 2000) and the degeneration pattern in PD (Bernheimer et al., 1973; Damier et al., 1999; Hirsch et al., 1988) and in our rat model of PD, the midbrain DA-formation was divided into three regions: (1) the SNcv, which includes A9 DA-cells lying in the ventrolateral region of the SN pars compacta and the SN pars reticulata; (2) the SNrm, and (3) VTA (see Fig. 1A). The striatum was divided into the dorsal striatum (dSt), whose DA-afferents come mainly from the SNcv, and the ventral striatum (vSt), whose DA-afferents come mainly from the SNrm and VTA (see Fig. 1D).

Cell count

The analysed parameters were: (1) number and localization of TH-cells three weeks after 6-OHDA injection, and (2) number and localization of TH-cells showing morphological features of neuronal degeneration (neuronal body swelling and FJ histofluorescence) 48 h after 6-OHDA injection. All studies were performed in 5 rats per group. We used the optical dissector method (West, 1999; Williams and Rakic, 1988) and a computer-assisted image analysis system attached to an Olympus microscope (BX51) equipped with a 40×, 0.75 N.A. objective, motorized stage with serial optical sections 2 μm apart in the z axis, and an Olympus camera (DP70). An electronic microcaptor (MT12) was connected to both the microscope and the parallel port of the computer. Cell counting was performed with the computer assisted stereological toolbox software (C.A.S.T.-grid) from Olympus, Denmark. Six 50-μm thick sections 150 μm apart from each other in the rostrocaudal axis were randomly selected in each rat. DA-regions were divided into fields of 150 × 125 μm at a magnification of 400×. Cell counts were performed in four randomly selected boxes of 75 μm (x-axis) × 62 μm (y-axis) × 20 μm (z-axis) per region and section.

Densitometric analysis of labelling intensity was performed in DAT-immunostained midbrain somata and in TH-immunostained striatal terminals. The study was performed on 5 rats per group, and six 25-μm thick sections 150 μm apart from each other per rat. In order to prevent

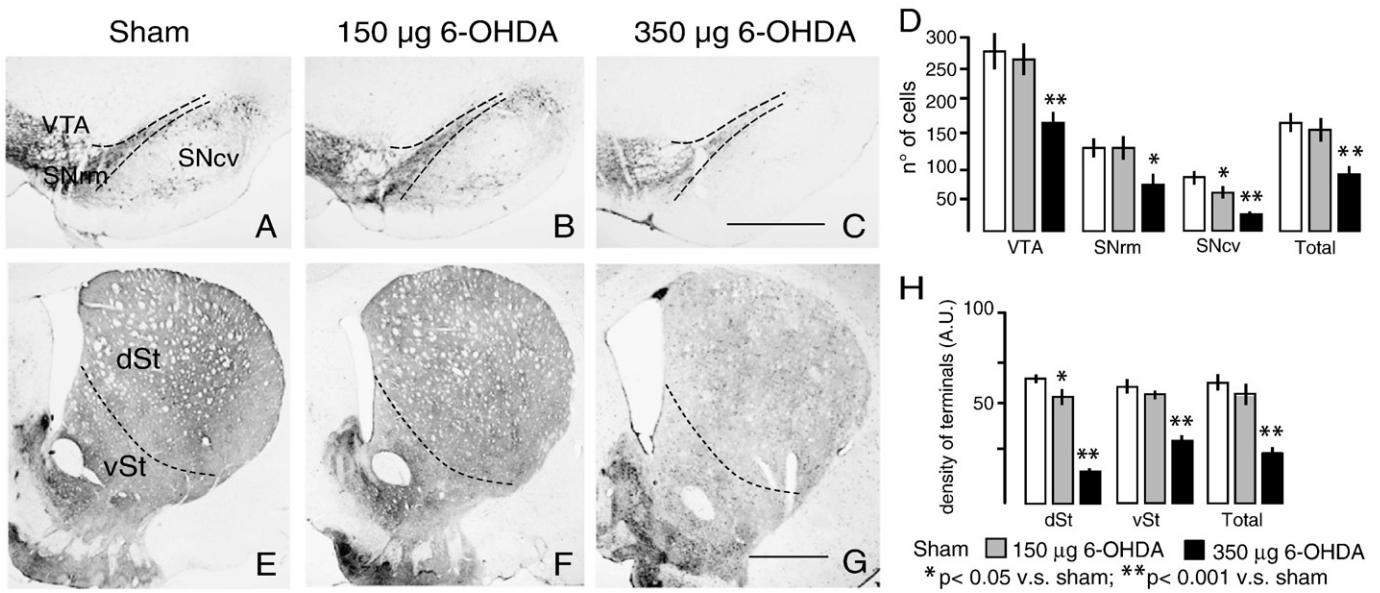

Fig. 1. Tyrosine hydroxylase immunohistochemistry and quantitative analysis showing the degeneration pattern of midbrain dopaminergic cells (A–D) and striatal terminals (E–H) in rats receiving sham (A, E), 150 µg 6-OHDA (B, F), and 350 µg 6-OHDA (C, G) intracereventricular injections. The loss of somata and terminals after 150 µg 6-OHDA injection is only significant in the SNcv and dSt, respectively. After 350 µg 6-OHDA injection, degeneration affects all mesostriatal divisions, but preferentially SNcv and dSt. dSt, dorsal striatum; SNcv, caudoventral region of the substantia nigra; SNrm, rostromedial region of the substantia nigra; vSt, ventral striatum; VTA, ventral tegmental area. Dashed lines indicate the putative borderline between VTA and SNrm, SNrm and SNcv, and dSt and vSt. Bar in C (for A–C) and in G (for E–G), 1 mm.

differences due to variations in protocol conditions during tissue processing and densitometric analysis the following precautions were taken: (1) different antibody dilutions were tested to establish the optimal work dilutions in the linear range of colorimetric intensity; (2) all sections were processed simultaneously using the same protocol and chemical reagents, and (3) all microscopic and computer parameters were kept constant throughout the densitometric study. At least 60 cells per nucleus and rat were analysed, and the labelling intensity of each cell was compared to that of the neighbouring background in axodendritic-stained free areas. The labelling intensity of the terminals was obtained from randomly selected 30 µm × 30 µm square areas located in dSt and vSt (15 areas per region and section, 6 sections per rat). The labelling intensity of each area was compared to that of the neighbouring corpus callosum. Microscopic images were digitised and the labelling intensity was analyzed using densitometry software (Leica Microsystems, Wetzlar, Germany). The labelling intensity was defined as the index of light attenuation with respect to the neighbouring background and expressed as arbitrary units (A.U, range 0–256).

In situ hybridization histochemistry

The antisense and the control sense rat digoxigenin-labelled DAT riboprobes used in this study were produced by *in vitro* transcription of DAT cDNA in a dual-promoter expression vector following the synthesis procedure previously described (Gonzalez-Hernandez et al., 2004). The DAT cDNA (700 bp) was from Dr. Martres (Martres et al., 1998). Details about DAT ISH labelling have also been previously described (Gonzalez-Hernandez et al., 2004; Cruz-Muros et al., 2009). The probe was added to the hybridization mix at 400 ng/ml. After posthybridization washes, the slides were incubated for 2 h at RT with alkaline-phosphatase conjugated anti-DIG monoclonal antibody (1:5000 final dilution in 100 mM TrisHCl, 150 mM NaCl pH 7.5 (TN) with 0.5% blocking reagent, Roche Diagnostics, Mannheim, Germany), and for 8 h in substrate (NBT and BCIP, Roche Diagnostics; 0.5%) in TNM buffer (100 mM TrisHCl, 100 mM NaCl, 50 mM MgCl2, pH 9.5). Some sections were processed for DAT mRNA-TH double fluorescent labelling. Briefly, after post-hybridization washes, they were incubated for 30 min in anti-digoxigenin-horseradish peroxidise (1:150, Roche Diagnostics, in 0.5% Blocking TSA in TN), and for 10 min in Biotinyl-tyramide (1:100; PerkinElmer; Shelton, CT). DAT ISH fluorescent labelling was visualized after incubation in Cy3-Extravidin (1:1000, Jackson-ImmunoResearch, West Grove, PA; in PBS). Thereafter, the sections were processed for TH immunohistochemistry by using mouse anti-TH monoclonal antibody (Sigma; 1:6,000) as primary antibody and fluorescein isothiocyanate-conjugated goat anti-mouse IgG (Sigma, 1: 100) as secondary antibody.

Quantitative RT-PCR, Western-blot analysis and synaptosomal [^{3}H]-DA uptake

These experiments were performed according to the protocol described by Cruz-Muros et al. (2009). For details see Supplementary material.

In vitro study

Plasmid constructs, mutagenesis and cell line transfection

Full-length rat DAT cDNA was obtained by RT-PCR from mRNA extracted from rat substantia nigra using a proof-reading DNA polymerase (Expand High Fidelity Kit, Roche Diagnostics). Specific primers were designed from the reported sequence (Genebank accession number NM_012694) and specific restriction sites were added to the 5'-and 3'-ends to facilitate cloning. Primer sequences were: rDAT-F: 5'-GGGGTACCCGCCACCATGAGTAAGAGCAAATGCTCCGTG-3' and rDAT-R: 5'-GGAATTCTTACAGCAACAGCCAGTGACGCAG-3'. The amplified fragment was cloned in pcDNA3.1(+)-neomycin (Invitrogen, Carlsbad, CA). The construct was sequenced at the University of La Laguna DNA sequencing facility.

HEK293 cells were maintained in Dulbecco's Modified Eagle's Medium (DMEM) supplemented with 10% fetal bovine serum, penicillin and streptomycin in a humidified incubator set at 37 °C and 5% CO_2. The cells were transfected with lipofectamine 2000 (Invitrogen)

following the manufacturer's instructions. Stable cell lines expressing rDAT were obtained by growth on selective medium containing 1 mg/ml of G418 (Invitrogen). After 10–12 days of selection in G418, individual clones were expanded in multi-well plates and examined for DAT expression by western blot and immunofluorescence. Several positive clones were identified and used for subsequent experiments.

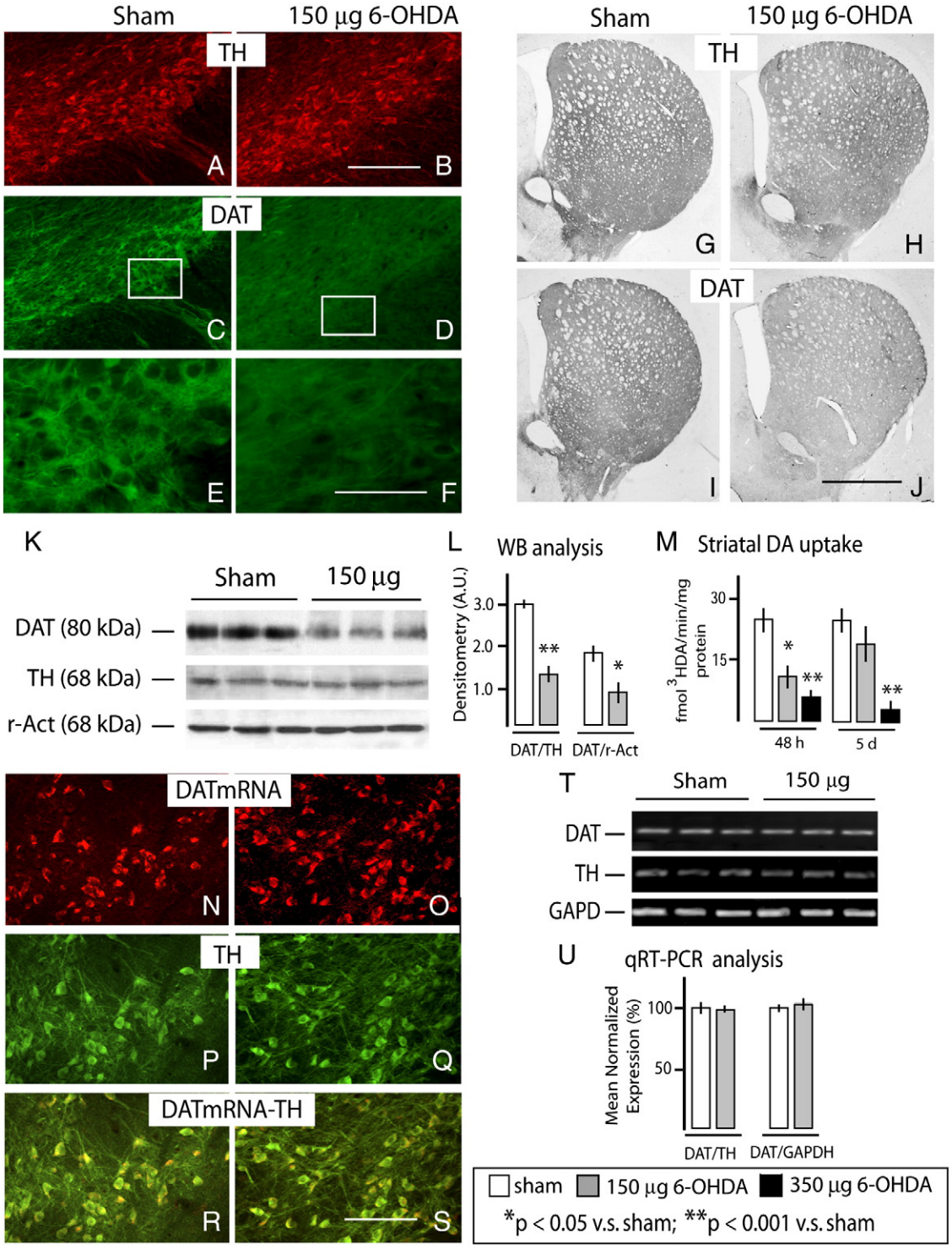

Fig. 2. Intracerebroventricular injection of 150 µg 6-OHDA induces post-traductional DAT down-regulation. (A–J) Immunostaining for TH (A, B, G and H) and glyco-DAT (C–F, I and J) in the substantia nigra (A–F) and striatum (G–J) 24 h after sham- (A, C, E, G and I) and 150 µg 6-OHDA- (B, D, F, H and J) injection. (E and F) boxed areas in C and D, respectively. We note a decrease in glyco-DAT- (D, F and J) but not in TH-immunostaining (B and H) in midbrain somata and striatum after 6-OHDA injection. (K and L) Western-blot analysis for glyco-DAT, TH and r-Actin of whole protein striatal extracts from sham- and 150 µg 6-OHDA-injected rats showing glyco-DAT expression decrease after 6-OHDA injection. (M) Striatal DA uptake 48 h and 5 days after injection in sham-, 150 µg 6-OHDA-, and 350 µg 6-OHDA-injected rats. DA uptake is transiently decreased at 48 h in 150 µg 6-OHDA injected rats, while in 350 µg 6-OHDA injected rats, DA uptake is persistently decreased after injection. (N–S) *In situ* hybridization for DAT mRNA, immunohistochemistry for TH, and double labelling for DAT mRNA and TH in the substantia nigra of sham (N, P and R) and 150 µg 6-OHDA (O, Q and S) injected rats showing that all midbrain DA-cells maintain DAT mRNA expression after 6-OHDA injection. (T and U) qRT-PCR for DAT, TH and GAPD showing no changes in DAT with respect to TH and GADP after 150 µg 6-OHDA injection. Bar in B (for A–D), 150 µm; in F (for E and F), 40 µm; in J (for (G–J), 1 mm; in S (for N–S), 80 µm.

[^{3}H]-DA uptake and cytotoxicity assays

DA uptake and cytotoxicity assays in HEK transfected cells were performed according to Storch et al. (1999) and Li et al. (2004). The cells were grown to confluence on 6-well dishes for [^{3}H]-DA uptake assay. They were dissociated with trypsin-EDTA, and after cell detaching, the trypsin action was immediately terminated by adding the same volume of DMEM. The cells were centrifugated at 1000 rpm for 2 min, washed twice and resuspended in assay buffer. Samples of 50 µl cell suspensions (1 µg total protein/µl) were analysed as described for synaptosomes in supplementary material.

The MTT (3[4,5-dimethylthiazol-2-yl]-2,5-diphenyltetrazolium bromide) assay was used to determine the vulnerability of cells to three different neurotoxins: MPP^+, the active metabolite of MPTP, whose toxic effect depends on DAT activity (Przedborski and Jackson-Lewis, 1998; Storch et al., 1999); 6-OHDA, whose toxic effect on cell culture, in contrast to that in experimental animals, is mediated by the generation of reactive oxygen species in the extracellular space rather than by transmembrane transport via catecholaminergic uptake (Storch et al., 2000; Woodgate et al., 1999), and rotenone, a lipophilic molecule able to penetrate all cell membranes and inhibit the mitochondrial respiratory chain (Betarbet et al., 2002; Marey-Semper et al., 1995). Cells were seeded in 24-well dishes at a density of 20,000 cells/well (in 400 µl medium) and grown for 48 h. The medium was then supplemented with ascorbic acid (0.022 mg/ml final concentration), and 24 h later different concentrations of MPP^+ (0 µM–1000 µM), 6-OHDA (0 µM–200 µM) or rotenone (0 µM–1000 µM) with and without nomifensine (17.7 µg/ml) were added. After incubation for 24 h at 37 °C, 100 µl of MTT reagent (0.5% MTT in PBS, 0.1% final concentration) was added to each well and incubated at 37 °C for 3 h. Thereafter, 400 µl of lysis buffer (20% w/v sodium dodecyl sulfate (SDS) in 50% *N,N*-dimethyl formamide, with 2.5% HCl and 2.5% 80% acetic acid, pH 4.7) was added and incubated overnight at 37 °C. The optical density of the samples was then measured at 570 nm with reference at 630 nm. MTT reduction was expressed as a percentage of the untreated wild-type HEK cells. The cytotoxic effect was also studied using morphological parameters. Changes in the DAT immunostaining pattern and the number of apoptotic nuclei were analysed.

Statistics

Mathematical analysis was performed using the one way ANOVA followed by the Tukey honest test for multiple post hoc comparisons. Analysis was performed using the Statistica program (Statsoft; Tulsa, U.S.A.). A level of $p<0.05$ was considered as critical for assigning

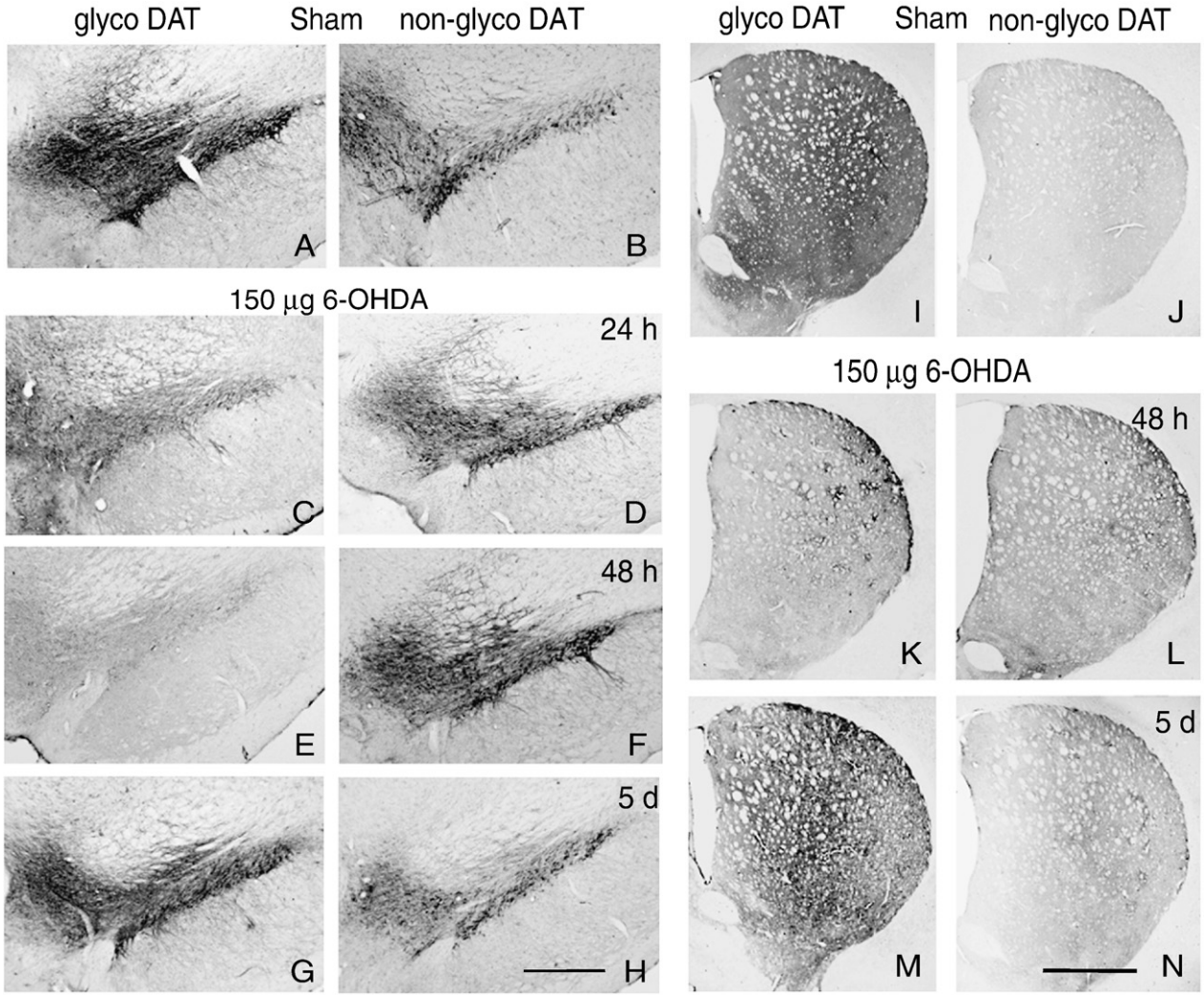

Fig. 3. Intracerebroventricular injection of 150 µg 6-OHDA induces a transient decrease in glyco DAT expression and a transient increase in non-glyco DAT expression in the mesostriatal system. Immunostaining for glyco-DAT and non-glyco DAT in the midbrain and striatum of sham- (A, B, I and J) and 150 µg 6-OHDA-injected rats at 24 h (C and D), 48 h (E, F, K and L) and 5 days (G, H, M and N) after injection. The immunostaining for glyco-DAT decreases and that for non-glyco DAT increases in both the ventral midbrain and striatum at 24–48 h after 6-OHDA injection. The normal pattern is recovered on the fifth day.

statistical significance. Data are expressed as mean ± standard error of the mean.

Results

DAT expression after i.c.v. injection of 6-OHDA in rats

As mentioned in material and methods, the rats were injected with either 150 μg or 350 μg 6-OHDA to study the effects of two different degrees of DA-lesion. After 150 μg injections, the number of TH-cells decreased in the SNcv (23%; $p<0.05$ vs. sham, $F=9.82$), but not in other midbrain DA-regions and the ventral midbrain as a whole (Fig. 1B and D). In addition, the degeneration of striatal DA-terminals, as revealed by TH immunohistochemistry densitometry, was only significant in the dSt (11%; $p<0.05$ vs. sham, $F=6.11$; Fig. 1F and H). After 350 μg injections, TH-cell degeneration affected 48% of the total number of midbrain DA-cells ($p<0.001$ vs. sham, $F=34,77$; Fig. 1C and D), and was preferentially localized in the SNcv, where it reached 71% ($p<0.001$ vs. sham, $F=30,34$). This 6-OHDA dose also caused an intense degeneration of striatal DA-terminals (62%), which was preferentially located in the dorsal striatum, where the loss of DA-terminals was about 78% with respect to the sham injected rats ($p<0.001$, $F=48,12$; Fig. 1G and H). DAT expression changes were observed in both experimental groups, although with differences in their time pattern of response.

DAT expression after 150 μg 6-OHDA injections

The use of antibodies that detect the glycosylated (mature, 75–80 kDa) DAT form (see DAT antibodies in supplementary material and supplementary fig. 1) revealed a decrease in DAT expression 24 h after 150 μg 6-OHDA injection. This effect was evident in midbrain DA-somata by using immunohistochemistry (Fig. 2A–F) and in striatal terminals by using immunohistochemistry and western-blot ($p<0.001$ vs. sham, $F=22.18$; Fig. 2G–L). Consistent with this finding, DA uptake was significantly reduced with respect to the sham injected group ($p<0.05$, $F=10.18$; Fig. 2M), but no changes were observed in DAT mRNA expression. As occurred in sham injected rats (Fig. 2N, P, R), all midbrain DA-cells were doubly labelled for DAT mRNA and TH in 150 μg 6-OHDA injected rats (Fig. 2O, Q, S), and qRT-PCR showed similar DAT mRNA levels in the ventral midbrain of both experimental groups (Fig. 2T and U).

Interestingly, in parallel with the decrease in glycosylated-DAT expression, the non-glycosylated (immature, 50 kDa) DAT form underwent a transient increase. At 24 h after lesion, and more markedly at 48 h, coinciding with the decrease in glyco-DAT (Fig. 3C and E), midbrain DA-cells and their axons in the medial forebrain fascicle were intensely stained for non-glyco DAT (Fig. 3D and F). Thereafter, glyco- and non-glyco-DAT turned back to their normal patterns, and were similar to that in sham injected rats 5 days after injection (Fig. 3G and H). These changes were also observed in the striatum. As shown in Fig. 3K and L, at 48 h after lesion, and coinciding with the glyco-DAT decrease, non-glyco-DAT expression increased in striatal terminals. Five days after lesion (Fig. 3M and N), the immunostaining for glyco- and non-glyco-DAT recovered their normal patterns.

DAT expression after 350 μg 6-OHDA injections

As mentioned above, these injections caused a marked DA-cell loss, with surviving neurons lying in VTA and SNrm (Fig. 4A) and projecting to the vSt (Fig. 4D). These neurons also underwent a reversal in their glyco-/non-glyco-DAT expression pattern. Midbrain somata and fibres and striatal terminals showed an increase in non-glyco-DAT expression (Fig. 4B and E) and a decrease in glyco-DAT expression (Fig. 4C and F). But, in contrast to 150 μg 6-OHDA injected rats, these changes persisted for at least three weeks after injection.

In summary, we can say that midbrain DA-neurons down-regulate DAT in response to an oxidative injury. This response is transient after a slight DA-lesion, and persistent after a strong DA-lesion. The evidence of a decrease in the expression of the glycosylated DAT form with no changes in DAT mRNA, and an increase in its non-glycosylated form, indicates that DAT down-regulation occurs at post-traslational level.

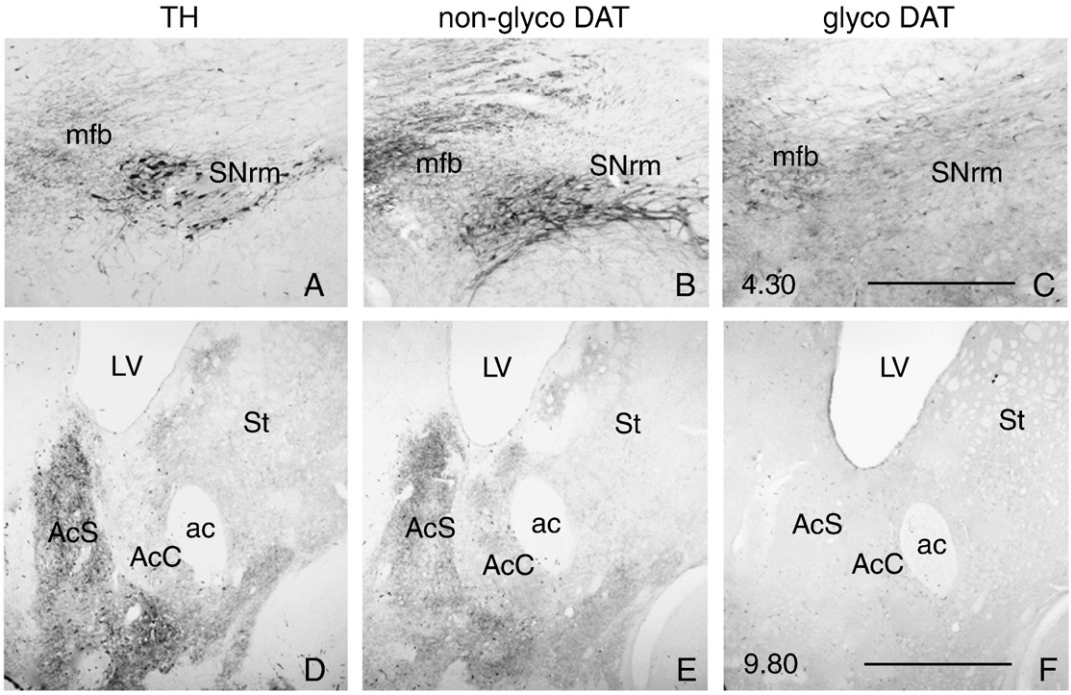

Fig. 4. DAT expression changes induced by 350 μg 6-OHDA injections in surviving mesostriatal neurons are persistent. Immunohistochemistry for TH (A and D), non-glyco DAT (B and E), and glyco-DAT (C and F) in the midbrain (A–C) and striatum (D–F) 3 weeks after injection. DA-cells in the SNrm and their terminals in the vSt show immunoreactivity for non-glyco DAT but not for glyco-DAT. ac, anterior commissure; AcC, accumbens nucleus, core; AcS, accumbens nucleus, shell; LV, lateral ventricle; mfb, medial forebrain bundle; St, striatum. Numbers in the lower left-hand corner in C and F indicate the approximate distance to the interaural line. Bar in C (for A–C), 250 μm; in F (for D–F), 1 mm.

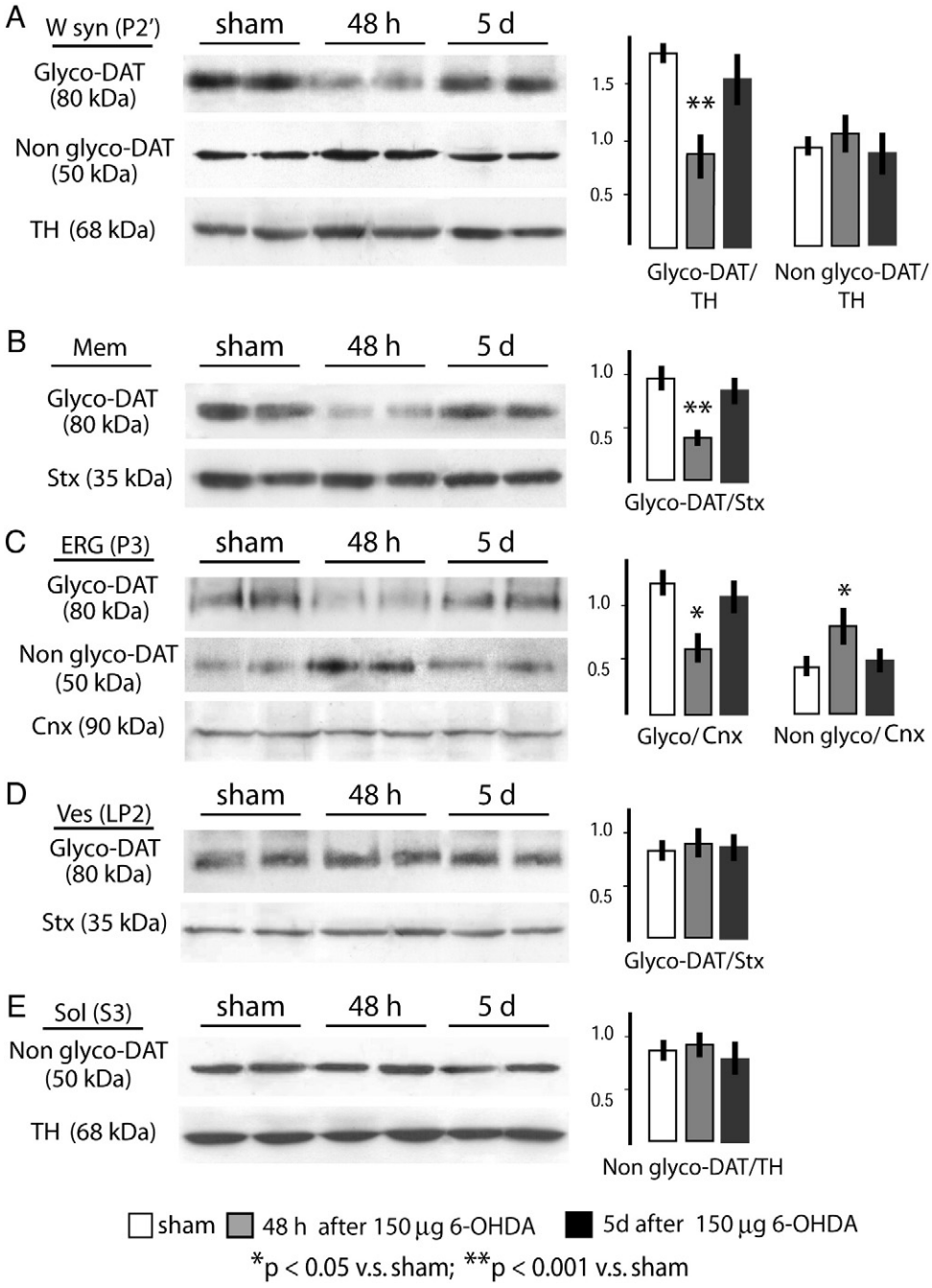

Fig. 5. Transient DAT down-regulation induced by 150 µg 6-OHDA injection consists of the decline in glyco-DAT expression in the synaptosomal membrane and accumulation of non-glyco DAT in the endoplamic reticulum-Golgi compartment. Western-blot for glyco-DAT and non-glyco DAT in whole synaptosomal extracts (A, W syn, P2'), and the plasma membrane (B, Mem), endoplasmic reticulum-Golgi (C, ERG, P3), vesicle (D, Ves, LP2) and soluble subcellular fractions (E, Sol, S3), in sham- and 150 µg 6-OHDA-injected rats 48 h and 5 days after injection. We note that glyco-DAT levels decrease in whole synaptosomes (A) and the plasma membrane (B) and endoplasmic reticulum-Golgi (ERG) compartments, and that non-glyco DAT levels increase in the ERG compartment 48 h after injection. The normal expression pattern is recovered on the fifth day.

Subcellular distribution of DAT after i.c.v. injection of 6-OHDA

These experiments were performed in 150 µg 6-OHDA injected rats because the degree of DA-lesion after 350 µg 6-OHDA injections made it difficult to obtain subcellular extracts for quantitative analysis. As shown in Fig. 5A, both DAT forms, glyco (80 kDa) and non-glyco (50 kDa), were detected in whole striatal synaptosomes (W syn, P2 fraction). By using r-Act (data not shown) and TH as house keeping

Fig. 6. DAT is redistributed from the plasma membrane to the endoplasmic reticulum in rDAT transfected HEK cells exposed to low concentrations of MPP^+. (A-C) Western-blot for DAT, DAT-DAPI double staining and DA uptake in untransfected cells (HEK) and in rDAT transfected cells (rDAT-HEK). HEK cells show very weak expression of non-glyco DAT (50 kDa) which is not detected in immunocytochemistry. rDAT-HEK cells show robust expression of glyco-DAT (80 kDa) which localizes in the plasma membrane and transports DA efficiently. (D–F) Toxic effect of MPP^+, 6-OHDA and rotenone on HEK- and rDAT-HEK-cells (with and without nominfensine (NMF) treatment) measured by MTT reduction. The half-maximal inhibitory concentration of MPP^+ toxicity (D) is much lower in rDAT-HEK cells (IC_{50} = 1.33 µM) than in HEK cells (IC_{50} = 976 µM) and rDAT-HEK cells treated with NMF (IC_{50} = 795 µM). The response to 6-OHDA (E) and rotenone (F) is similar in both cell phenotypes and not affected by NMF treatment. (G–P) Differential effect of MPP^+, 6-OHDA and rotenone on the subcellular distribution of DAT and cell viability. Left column, DAT-DAPI double staining; right column, DAT-DAPI-calnexin (CNX) triple staining. We can see that 24 h after incubation in 0.3 µM MPP^+ (I and J) DAT expression decreases in the plasma membrane and colocalizes with CNX, while after exposure to higher concentration of MPP^+ (10 µM; K and L) and low concentrations of 6-OHDA (25 µM; M and N) or rotenone (1 µM; O and P), many neurons display an apoptotic nucleus and DAT is maintained in the plasma membrane.

proteins, we found a decrease of 55% in the synaptosomal expression of glyco-DAT 48 h after lesion ($p<0.001$ vs. sham; $F=19.20$), with the return to the normal levels on the fifth day, and no significant changes in non-glyco-DAT expression. The synaptosomal membrane fraction (avidin-absorbed biotinylated surface proteins) showed one single band at ~80 kDa (Fig. 5B, Mem), suggesting that the glycosylated DAT form is the only or the predominant form in DA-terminal membranes. In parallel to that found in whole synaptomes, the densitometric analysis using syntaxin (Stx) as a marker of plasma membrane, showed a significant decrease (63%; $p<0.001$ vs. sham; $F=22.4$) in DAT

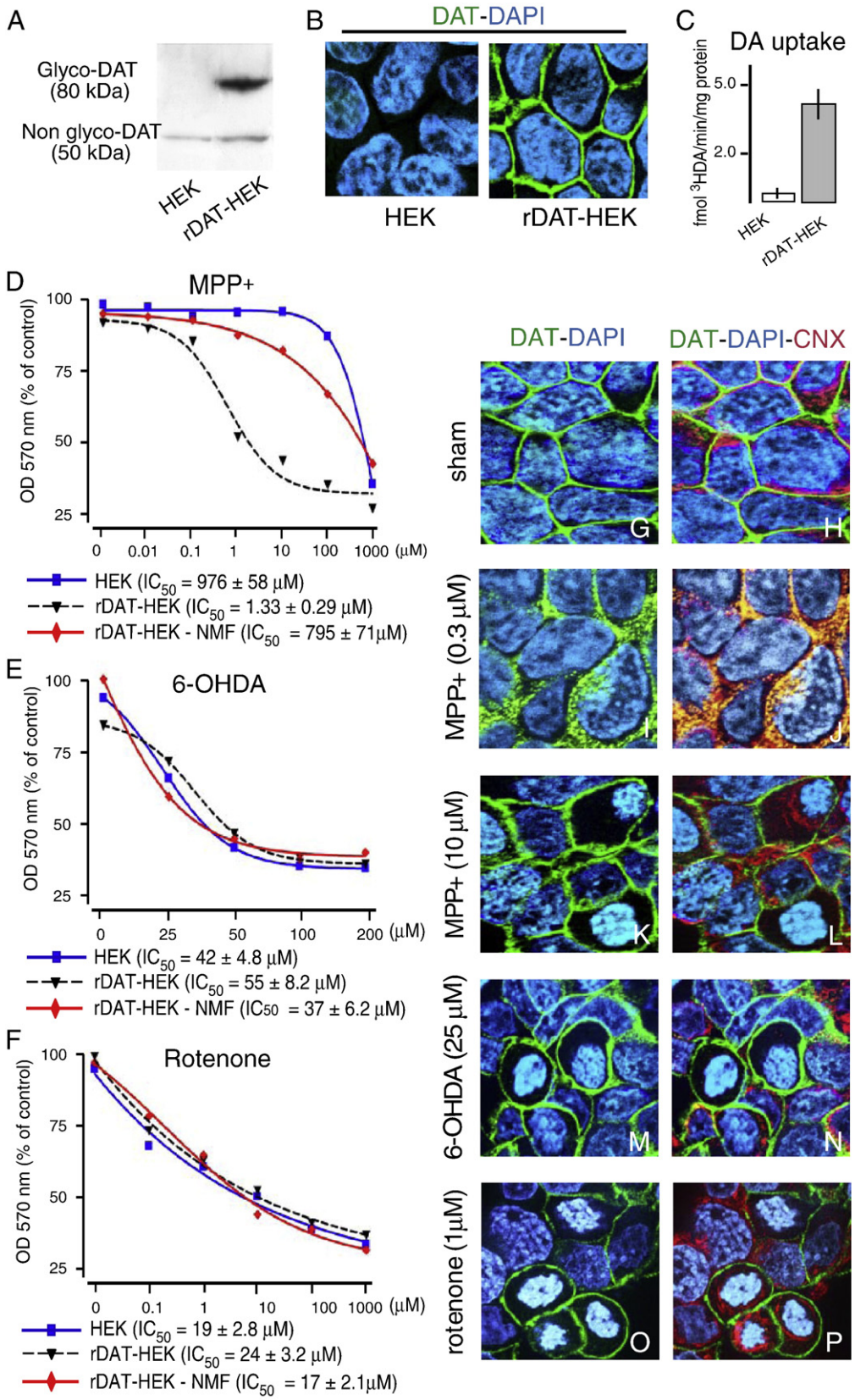

expression 48 h after 6-OHDA injection, and its recovery on the fifth day. As shown in Fig. 5C, both glyco- and non-glyco DAT were detected in the endoplasmic reticulum-Golgi complex (ERG, P3 fraction), with the glycosylated form displaying a higher expression than the non-glycosylated one in sham injected rats. This expression pattern was modified 48 h after 6-OHDA injection, with a decrease in glycosylated DAT (49%, $p<0.05$ vs. sham; $F=14.91$) and an increase in non-glycosylated DAT (71%, $p<0.05$ vs. sham; $F=11.82$). The expression of both forms returned to the normal pattern by day 5 post-lesion. The vesicle-enriched fraction showed a prominent band at 80 kDa (Fig. 5D; Ves, LP2), but the density at 50 kDa was very low making the densitometric analysis impossible (data not shown). The striatal soluble fraction, on the contrary, only showed a solid band at 50 kDa (Fig. 5E; Sol, S3). DAT expression in both subcellular fractions showed no significant changes after 6-OHDA injection.

Subcellular distribution of DAT in response to MPP$^+$, 6-OHDA and rotenone in rDAT transfected HEK cells

The results described above indicate that DAT is transiently redistributed from the plasma membrane to the ERG compartment in response to 6-OHDA injection in rats. Bearing in mind that the neurotoxic effect of 6-OHDA injections depends on the activity of DAT, we investigated the possibility that DAT redistribution is also induced by DAT-independent neurotoxins. These experiments were performed in rDAT stably transfected HEK-293 cells (rDAT-HEK cells) exposed to three different neurotoxins: MPP$^+$, the active metabolite of MPTP, whose toxic effect depends on DAT activity (Przedborski and Jackson-Lewis, 1998; Storch et al., 1999); 6-OHDA, whose toxic effect on cell culture, in contrast to that in experimental animals, is mediated by the generation of reactive oxygen species in the extracellular space rather than by transmembrane transport via catecholaminergic uptake (Storch et al., 2000; Woodgate et al., 1999), and rotenone, a lipophilic molecule with capacity to penetrate all cell membrane and inhibit the mitochondrial respiratory chain (Betarbet et al., 2002; Marey-Semper et al., 1995). Western-blot for DAT in rDAT-HEK cells showed a broad band at 80 kDa and a thinner band at 50 kDa, whereas in non-transfected HEK cells, or in cells transfected with the empty vector (data not shown), only a thin band at 50 kDa was detected (Fig. 6A, B). DA uptake assay revealed a high degree of DAT activity in rDAT-HEK cells, whereas the endogenous levels of DAT in non-transfected cells were not high enough to provide significant DA uptake under the experimental conditions used in this study (Fig. 6C).

As shown in the MTT assay (Fig. 6D–F), the toxicity of MPP$^+$ on non-transfected HEK cells was obtained at practically the mM concentration range ($IC_{50}=976\pm58$ μM), while in rDAT-HEK cells it was obtained around 1.0 μM ($IC_{50}=1.33\pm0.29$ μM), and inhibited by coincubation with nomifensine ($IC_{50}=795\pm71$ μM; Fig. 6D). The toxicity of 6-OHDA and rotenone on non-transfected cells ($IC_{50}=42\pm4.8$ μM and 19 ± 2.8 μM, respectively) were similar to those in rDAT-HEK cells ($IC_{50}=55\pm8.2$ μM and 22 ± 3.2 μM, respectively), and not affected by nomifensine (Fig. 6E and F). Calnexin was used as a marker of the endoplasmic reticulum-Golgi compartment in the microscopic analysis of DAT subcellular distribution. Under normal conditions, DAT labelling localizes in the plasma membrane of rDAT-HEK cells (Fig. 6G and H). After incubation in 0.3 μM MPP$^+$ for 24 h, DAT labelling becomes intracellular and granular in shape, and colocalizes with calnexin in most rDAT-HEK cells (Fig. 6I and J), and the count of apoptotic nuclei showed no differences with untreated cells ($0.4\pm0.07\%$). After incubation in 10 μM MPP$^+$, DAT labelling was maintained in the plasma membrane of most cells, and many nuclei ($18\pm1.6\%$) became apoptotic (Fig. 6K and L). In the case of 6-OHDA and rotenone, DAT redistribution was not observed, but an increased number of apoptotic nuclei ($21\pm2.2\%$ and $16\pm2.0\%$ respectively) was clearly evident even at low concentration ranges of the neurotoxins (25 μM 6-OHDA and 1 μM rotenone; Fig. 6M–P).

Differences in DAT regulation and vulnerability in midbrain DA-cells

The analysis of glyco-DAT immunostaining in 150 μg 6-OHDA injected rats showed differences in the pattern of DAT-expression changes between DA-cells in the SNrm and SNcv. It should be noted that in sham injected rats (Fig. 7A–C, N), as previously reported in intact rats (Gonzalez-Hernandez et al., 2004), the labelling intensity for glyco-DAT in SNcv neurons was slightly but significantly higher ($23.8\pm4.1\%$; $p<0.001$ vs. SNrm; $F=17.04$) than in SNrm neurons. Twenty-four hours after 6-OHDA injection this difference was higher. The labelling intensity in SNrm DA-cells decreased to $35.2\pm6.3\%$ of that in the sham rats ($p<0.001$; $F=35.19$), whereas in the SNcv, the labelling intensity was maintained at $79.3\pm8.0\%$ of that in the sham group ($p<0.05$; $F=12.33$), that approximately corresponds to the densitometric value of SNrm DA-cells in sham rats (Fig. 7D–G, N). Interestingly, 24 h later (48 h after 6-OHDA injection), $24.7\pm4.2\%$ DA-cells in the SNcv showed swelling (Fig. 7I, arrows), dendritic fragmentation and Fluoro-Jade fluorescence (Fig. 7J), whereas only $5.8\pm1.3\%$ of those the SNrm displayed signs of degeneration ($p<0.001\%$ vs. SNcv; $F=41.3$; Fig. 7O), suggesting a relationship between DAT down-regulation and neuroprotection. The decline of glyco-DAT expression also displayed topographic differences at terminal level. In contrast to the robust loss of immunoreactivity in the vSt and the matriceal compartment of dSt, glyco-DAT staining was maintained in the striosomes (Gerfen, 1985; Graybiel et al., 1990) in the lateral region of the dSt, and throughout the subcallosal streak on the dorsolateral border of the striatum (Fig 7K–M). However, TH immunostaining revealed no differences in the intensity of terminal loss between the striosomal and matriceal compartments.

Discussion

In sum, our results show that DAT is down-regulated in response to dopaminergic lesion. This effect is transient in rats receiving 150 μg 6-OHDA i.c.v. injections, whose dopaminergic degeneration is restricted to a few neurons in the SNcv, and persistent after 350 μg 6-OHDA injections, whose degeneration affects about 50% of midbrain DA-cells. As shown in 6-OHDA injected rats and rDAT-HEK cells exposed to MPP$^+$, DAT is deglycosylated and redistributed from the plasma membrane to the endoplasmic reticulum-Golgi compartment, without changes in DAT mRNA levels. In contrast to DA-cells in the VTA and SNrm, those in SNcv do not regulate DAT after low doses of 6-OHDA and degenerate shortly after injection.

DAT is persistently down-regulated after striatal DA depletion

The decrease in DAT expression could be considered an expected finding after dopaminergic lesion since it is a direct consequence of DA-cell loss. However, data from *in vivo* (Bezard et al., 2001; Stachowiak et al., 1987) and *in vitro* studies (Berman et al., 1996; Chagkutip et al., 2003; Fleckenstein et al., 1997a; Gulley et al., 2002) show that the decline in DA uptake is higher than that expected in light of the extent of the lesion, suggesting that DAT is down-regulated. Our results in 350 μg 6-OHDA injected rats, whose degeneration reaches 62% of DA-terminals, reveal that surviving neurons maintain a decreased expression of functional (glycosylated) DAT for at least three weeks. Bearing in mind that the definitive 6-OHDA lesion is established in the first week after injection (Rodriguez et al., 2001b), the decrease in DAT expression should not be a direct effect of the neurotoxin. As with other phenomena occurring after striatal DA depletion, such as the increase in DA release and turnover (Robinson et al., 1994; Zigmond et al., 1990), and the hypersensitivity of

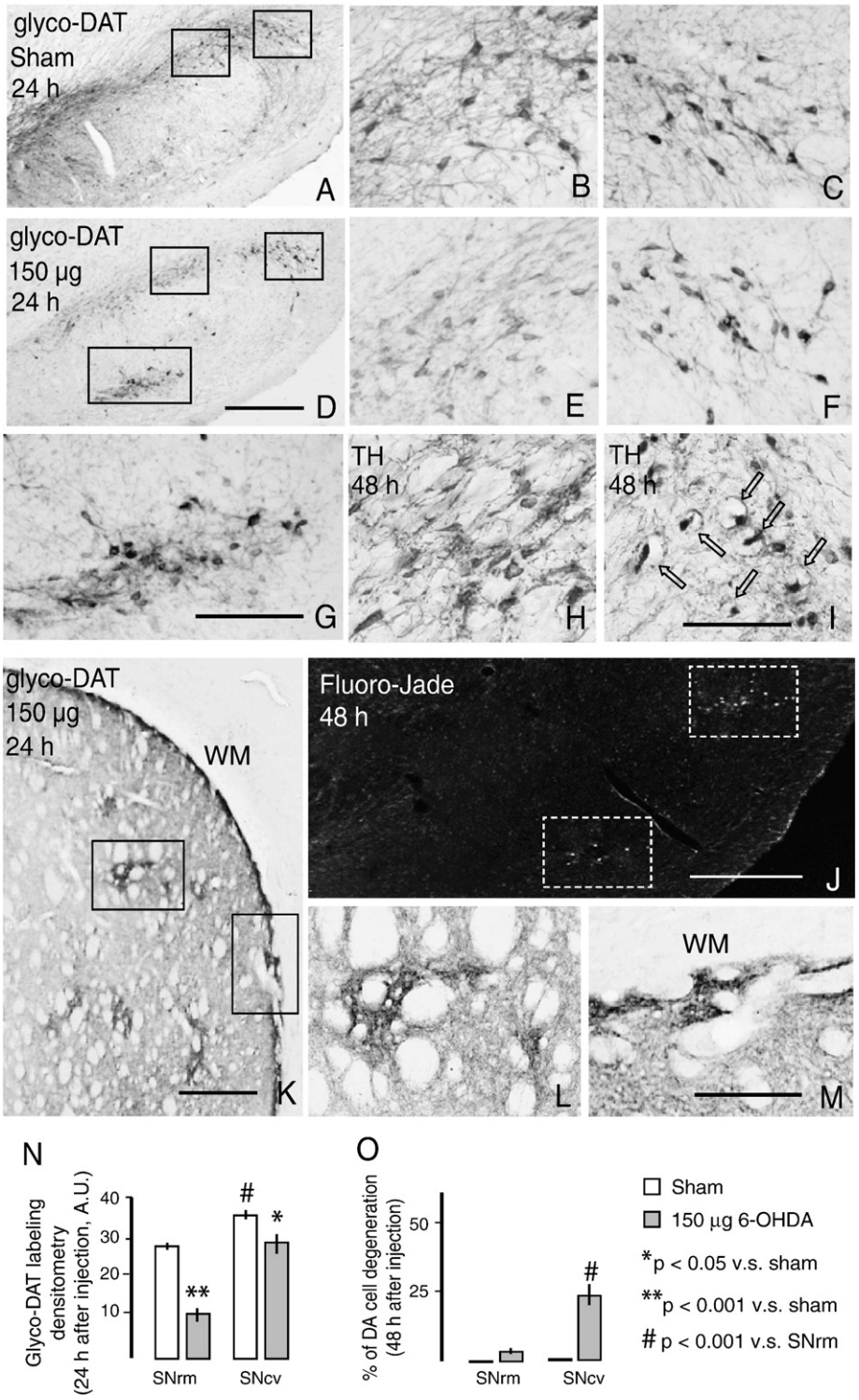

Fig. 7. DA-neurons in the ventrolateral region of the substantia nigra (SN) do not regulate DAT and degenerate shortly after 150 µg 6-OHDA injection. (A–G) Immunohistochemitry for glyco-DAT in the SN of sham- (A–C) and 6-OHDA- (D–G) injected rats 24 h after injection. (B and C) boxed areas in the upper middle and upper right-hand corner respectively in A. (E–G) boxed areas in the top middle, upper right-hand corner, and the bottom middle respectively in B. (H and I) TH immunohistochemistry of the dorsal and lateral regions of the SN, corresponding to those in E and F, respectively, 48 h after 6-OHDA injection. (J) Fluoro-Jade staining in the SN 48 h after 6-OHDA injection. Boxed areas enclose degenerated cells in the lateral and ventral regions of the SN. (K–M) Glyco-DAT immunohistochemistry in the striatum 24 h after 6-OHDA injection. (L and M) boxed areas in the middle and on the left-hand side, respectively, in K. (N) Densitometric analysis for glyco-DAT labelling in DA cells in the SNrm and SNcv 24 h after injection. (O) Count of DA-cells showing signs of degeneration (soma swelling and dendritic fragmentation) in the SNrm and SNcv 48 h after injection. We can see that the decrease in glyco-DAT expression in SNcv DA-cells 24 h after 150 µg 6-OHDA injection is lower than in the SNrm DA-cells (compare C with F and G, and B with E; N), and glyco-DAT labelling is maintained in the striosomes and subcallosal streak of the striatum (K–M). The following day (48 h after injection), many neurons in the SNcv show signs of degeneration (arrows in I and boxed areas in J) while most of these in the SNrm remain intact (H and O). WM, subcortical white matter. Bar in D (for A and D), 500 µm; in G (for B, C, E–G), 160 µm; in I (for H and I), 80 µm; in J, 500 µm; in K, 450 µm; in M (for L and M), 200 µm.

postsynaptic DA receptors (Bezard et al., 2003), DAT down-regulation is probably a long-term compensatory mechanism directed at maintaining DA input in the striatum.

A slight DA-injury induces transient DAT accumulation in the ERG compartment

DAT is also down-regulated in 150 μg 6-OHDA injected rats, whose dopaminergic lesion is virtually irrelevant, and in rDAT-HEK cells exposed to MPP^+ concentrations that induce minimal toxicity. Therefore, substantial dopaminergic lesion is not required for inducing DAT down-regulation. It is known that the activation of protein kinase C induces DAT internalization and DA uptake decline (Daniels and Amara, 1999; Zhu et al., 1997). Internalized DAT may be recycled back to the plasma membrane through an endosomal pathway (Melikian and Buckley, 1999), or sent to the lysosomal compartment to be degraded within 2 h after enzymatic activation (Daniels and Amara, 1999). Methamphetamine also induces an acute protein kinase C-dependent decrease in striatal DAT activity, which returns to control levels 24 h later (Fleckenstein et al., 1997b; Sandoval et al., 2001). The redistribution pattern of DAT in 150 μg 6-OHDA injected rats clearly differs from this. We found a decrease in glyco-DAT expression in the plasma membrane and an increase of non-glyco-DAT in the ERG compartment at 24–48 h after lesion, with recovery of the normal expression pattern and DAT activity 5 days after lesion. The absence of expression changes in the endosomal (vesicular) compartment together with the accumulation of non-glyco-DAT in the ERG compartment, suggest a stop or slowing in its maturation and trafficking to the plasma membrane. Immature DAT accumulated in the ERG could be degraded by the ubiquitin-proteosome system with the participation of multiple chaperones, as reported for other transmembrane proteins (Nakatsukasa et al., 2008). According to previous studies about the synthesis and turnover rates of monoamine transporters (Fleckenstein et al., 1996; Kimmel et al., 2000; 2001), the fact that functional expression is restored on the third day after its maximal decrease (5 days after injection) indicates that it probably comes from synthesis *de novo*.

Transient DAT down-regulation is induced by DAT-dependent neurotoxins

The exposure of rDAT-HEK cells to different neurotoxins revealed DAT redistribution without significant impairment of cell viability only after exposure to a low concentration of the DAT-dependent toxin MPP^+. Rotenone, a lipophilic neurotoxin that, similar to MPP^+, inhibits the mitochondrial complex I (Betarbet et al., 2002; Marey-Semper et al., 1995), and 6-OHDA which in cell culture, in contrast to that in animal models of PD, generates reactive oxygen species in the extracellular space rather than intracellularly (Storch et al., 2000; Woodgate et al., 1999), they both produced similar cytotoxicity in rDAT transfected- and untransfected-cells, and apoptosis without affecting DAT subcellular distribution. The fact that down-regulation was observed in 6-OHDA injected rats and MPP^+ exposed rDAT-HEK cells, but not in rotenone- and 6-OHDA-exposed rDAT-HEK cells, suggests a DAT-dependent effect. However, other possibilities cannot be ruled out because 6-OHDA and MPP^+ share other cytotoxic actions (Blum et al., 2001; Schober, 2004) that could be involved in this effect.

Transient DAT down-regulation is a neuroprotective mechanism

Our results show that while DA-neurons in the VTA and SNrm down-regulate DAT, many of those in the SNcv do not regulate DAT. Furthermore, DA-terminals in the vSt and the matrix of dSt regulate DAT, and those in the striosomes of dSt and the subcallosal streak do not regulate DAT. Hodological studies show that the vSt and the matriceal compartment of dSt are the main target of VTA and SNrm afferents, and that the striosomes and the subcallosal streak are the main target of those from the SNcv (Gerfen et al., 1987; Langer and Graybiel, 1989). So, there is a correspondence between somata and terminals which either regulate or do not regulate DAT. Interestingly, DA-somata which do not regulate DAT degenerate shortly after 150 μg 6-OHDA lesion, and those which regulate DAT remain intact, suggesting a relationship between DAT down-regulation and neuroprotection. However, this finding was not paralleled by differences in the intensity of terminal loss between the striosomal and matriceal compartments. It should be noted that preferential degeneration of striosomal terminals had been reported after injection of low doses of MPTP in marmosets (Iravani et al., 2005) and 3,4-methylenedioxymethamphetamine in mice (Granado et al., 2008). The DA-cell loss in these studies ranged between 25% and 40% of the total number of DA-cells, while in 150 μg 6-OHDA injected rats, degeneration was minimal. This was evident only on the basis of morphological aspects (swelling of cell somata and FJ fluorescence). Thus, striosomes can maintain their DA-afferents arising from preserved SNcv neurons, making it difficult to find regional differences in the density of terminals.

In conclusion, we propose a ventrolateral to dorsomedial gradient in the capability for regulating DAT in response to a dopaminergic injury. The lowest capability is in DA-cells in the ventrolateral region of the SNcv, which in spite of being the most distant ones from the third ventricle, and therefore exposed to lower 6-OHDA concentrations than any other DA-cell in the SN and VTA, do not regulate DAT and die after 150 μg 6-OHDA injections. The highest regulatory capability is in many DA-cells in the VTA and SNrm, which being close to the third ventricle, and exposed to the highest 6-OHDA concentrations, regulate DAT and remain intact after 350 μg 6-OHDA injection. Most DA-cells in SNrm and the medial region of SNcv display an intermediate ability for regulating DAT. They down-regulate DAT transiently after 150 μg 6-OHDA injections, but are unable to do this after 350 μg 6-OHDA injection. This behaviour is also observed in rDAT-HEK cells exposed to low and high concentrations of MPP^+. Bearing in mind that the DA-cell loss in PD also starts in the ventrolateral region of the SN and advances dorsomedially (Damier et al., 1999; Fearnley and Lees, 1991), differences in DAT regulation might be involved in the differential vulnerability and progression of DA-degeneration in this disease. On the other hand, it is known that the damaging effect of DAT is counteracted by the vesicular monoamine transporter type 2 (VMAT2). This is responsible for the vesicular storing of monoamines, exerting a protective effect by preventing interaction of DA with its enzymatic machinery (Wang et al., 1997; Gainetdinov et al., 1998a). Given that VMAT2 may also be regulated by dopaminergic insult (Chen et al., 2008), it would be interesting to investigate whether, similar to DAT, VMAT2 regulation contributes to the differential vulnerability of midbrain DA-cells.

Acknowledgments

This work was supported by Ministerio de Ciencia e Innovación (grant no. BFU2007-66561), Fundación Canaria de Invetigación y Salud (grant no 71/07), CIBERNED (ISCIII) and Instituto de Tecnologías Biomédicas.

Appendix A. Supplementary data

Supplementary data associated with this article can be found, in the online version, at doi:10.1016/j.nbd.2010.07.012.

References

Adams Jr., J.D., Chang, M.L., Klaidman, L., 2001. Parkinson's disease—redox mechanisms. Curr. Med. Chem. 8, 809–814.
Amara, S.G., Kuhar, M.J., 1993. Neurotransmitter transporters: recent progress. Ann Rev Neurosci 16, 73–93.

Berman, S.B., Zigmond, M.J., Hastings, T.G., 1996. Modification of dopamine transporter function: effect of reactive oxygen species and dopamine. J. Neurochem. 67, 593–600.
Bernheimer, H., Birkmayer, W., Hornykiewicz, O., Jellinger, K., Seitelberger, F., 1973. Brain dopamine and the syndromes of Parkinson and Huntington. Clinical, morphological and neurochemical correlations. J. Neurol. Sci. 20, 415–455.
Betarbet, R., Sherer, T.B., Greenamyre, J.T., 2002. Animal models of Parkinson's disease. Bioessays 24, 308–318.
Bezard, E., Dovero, S., Prunier, C., Ravenscroft, P., Chalon, S., Guilloteau, D., Crossman, A.R., Bioulac, B., Brotchie, J.M., Gross, C.E., 2001. Relationship between the appearance of symptoms and the level of nigrostriatal degeneration in a progressive 1-methyl-4-phenyl-1, 2, 3, 6-tetrahydropyridine-lesioned macaque model of Parkinson's disease. J. Neurosci. 21, 6853–6861.
Bezard, E., Gross, C.E., Brotchie, J.M., 2003. Presymptomatic compensation in Parkinson's disease is not dopamine-mediated. Trends Neurosci. 26, 215–221.
Bezard, E., Gross, C.E., Fournier, M.C., Dovero, S., Bloch, B., Jaber, M., 1999. Absence of MPTP-induced neuronal death in mice lacking the dopamine transporter. Exp. Neurol. 155, 268–273.
Blum, D., Torch, S., Lambeng, N., Nissou, M., Benabid, A.L., Sadoul, R., Verna, J.M., 2001. Molecular pathways involved in the neurotoxicity of 6-OHDA, dopamine and MPTP: contribution to the apoptotic theory in Parkinson's disease. Prog. Neurobiol. 65, 135–172.
Cerruti, C., Walther, D.M., Kuhar, M.J., Uhl, G.R., 1993. Dopamine transporter mRNA expression is intense in rat midbrain neurons and modest outside midbrain. Brain Res. Mol. Brain Res. 18, 181–186.
Cruz-Muros, I., Afonso-Oramas, D., Abreu, P., Perez-Delgado, M.M., Rodriguez, M., Gonzalez-Hernandez, T., 2009. Aging effects on the dopamine transporter expression and compensatory mechanisms. Neurobiol. Aging 30, 973–986.
Chagkutip, J., Vaughan, R.A., Govitrapong, P., Ebadi, M., 2003. 1-Methyl-4-phenylpyridinium-induced down-regulation of dopamine transporter function correlates with a reduction in dopamine transporter cell surface expression. Biochem Bioph Res Co 311, 49–54.
Chen, M.K., Kuwabara, H., Zhou, Y., Adams, R.J., Brasic, J.R., McGlothan, J.L., Verina, T., Burton, N.C., Alexander, M., Kumar, A., Wong, D.F., Guilarte, T.R., 2008. VMAT2 and dopamine neurons loss in a primate model of Parkinson's disease. J. Neurochem. 105, 78–90.
Damier, P., Hirsch, E.C., Agid, Y., Graybiel, A.M., 1999. The substantia nigra of the human brain. II. Patterns of loss of dopamine-containing neurons in Parkinson's disease. Brain 122 (Pt 8), 1437–1448.
Daniels, G.M., Amara, S.G., 1999. Regulated trafficking of the human dopamine transporter. Clathrin-mediated internalization and lysosomal degradation in response to phorbol esters. J. Biol. Chem. 274, 35794–35801.
Fallon, J.H., Moore, R.Y., 1978. Catecholamine innervation of the basal forebrain. IV. Topography of the dopamine projection to the basal forebrain and neostriatum. J. Comp. Neurol. 180, 545–580.
Fearnley, J.M., Lees, A.J., 1991. Ageing and Parkinson's disease: substantia nigra regional selectivity. Brain 114 (Pt 5), 2283–2301.
Fleckenstein, A.E., Kopajtic, T.A., Boja, J.W., Carroll, F.I., Kuhar, M.J., 1996. Highly potent cocaine analogs cause long-lasting increases in locomotor activity. Eur. J. Pharmacol. 311, 109–114.
Fleckenstein, A.E., Metzger, R.R., Beyeler, M.L., Gibb, J.W., Hanson, G.R., 1997a. Oxygen radicals diminish dopamine transporter function in rat striatum. Eur. J. Pharmacol. 334, 111–114.
Fleckenstein, A.E., Metzger, R.R., Wilkins, D.G., Gibb, J.W., Hanson, G.R., 1997b. Rapid and reversible effects of methamphetamine on dopamine transporters. J. Pharmacol. Exp. Ther. 282, 834–838.
Gainetdinov, R.R., Fumagalli, F., Jones, S.R., Caron, M.G., 1997. Dopamine transporter is required for in vivo MPTP neurotoxicity: evidence from mice lacking the transporter. J. Neurochem. 69, 1322–1325.
Gainetdinov, R.R., Fumagalli, F., Wang, Y.M., Jones, S.R., Levey, A.I., Miller, G.W., Caron, M.G., 1998a. Increased MPTP neurotoxicity in vesicular monoamine transporter 2 heterozygote knockout mice. J. Neurochem. 70, 1973–1978.
Gainetdinov, R.R., Jones, S.R., Fumagalli, F., Wightman, R.W., Caron, M.G., 1998b. Re-evaluation of the role of the dopamine transporter in dopamine system homeostasis. Brain Res Bras Res Rev 26, 148–153.
Gerfen, C.R., 1985. The neostriatal mosaic. I. Compartmental organization of projections from the striatum to the substantia nigra in the rat. J. Comp. Neurol. 236, 454–476.
Gerfen, C.R., Herkenham, M., Thibault, J., 1987. The neostriatal mosaic: II. Patch- and matrix-directed mesostriatal dopaminergic and non-dopaminergic systems. J. Neurosci. 7, 3915–3934.
Giros, B., Caron, M.G., 1993. Molecular characterization of the dopamine transporter. Trends Pharmacol. Sci. 14, 43–49.
Gonzalez-Hernandez, T., Barroso-Chinea, P., De La Cruz Muros, I., Del Mar Perez-Delgado, M., Rodriguez, M., 2004. Expression of dopamine and vesicular monoamine transporters and differential vulnerability of mesostriatal dopaminergic neurons. J. Comp. Neurol. 479, 198–215.
Granado, N., Escobedo, I., O'Shea, E., Colado, I., Moratalla, R., 2008. Early loss of dopaminergic terminals in striosomes after MDMA administration to mice. Synapse 62, 80–84.
Graybiel, A.M., Moratalla, R., Robertson, H.A., 1990. Amphetamine and cocaine induce drug-specific activation of the c-fos gene in striosome-matrix compartments and limbic subdivisions of the striatum. P Natl Acad Sci USA 87, 6912–6916.
Gulley, J.M., Doolen, S., Zahniser, N.R., 2002. Brief, repeated exposure to substrates down-regulates dopamine transporter function in Xenopus oocytes in vitro and rat dorsal striatum in vivo. J. Neurochem. 83, 400–411.
Hirsch, E., Graybiel, A.M., Agid, Y.A., 1988. Melanized dopaminergic neurons are differentially susceptible to degeneration in Parkinson's disease. Nature 334, 345–348.
Hurd, Y.L., Pristupa, Z.B., Herman, M.M., Niznik, H.B., Kleinman, J.E., 1994. The dopamine transporter and dopamine D2 receptor messenger RNAs are differentially expressed in limbic- and motor-related subpopulations of human mesencephalic neurons. Neuroscience 63, 357–362.
Iravani, M.M., Syed, E., Jackson, M.J., Johnston, L.C., Smith, L.A., Jenner, P., 2005. A modified MPTP treatment regime produces reproducible partial nigrostriatal lesions in common marmosets. Eur. J. Neurosci. 21, 841–854.
Joel, D., Weiner, I., 2000. The connections of the dopaminergic system with the striatum in rats and primates: an analysis with respect to the functional and compartmental organization of the striatum. Neuroscience 96, 451–474.
Kimmel, H., Vicentic, A., Kuhar, M.J., 2001. Neurotransmitter transporters synthesis and degradation rates. Life Sci. 68, 2181–2185.
Kimmel, H.L., Carroll, F.I., Kuhar, M.J., 2000. Dopamine transporter synthesis and degradation rate in rat striatum and nucleus accumbens using RTI-76. Neuropharmacology 39, 578–585.
Kopin, I.J., 1992. Features of the dopaminergic neurotoxin MPTP. Ann. NY Acad. Sci. 648, 96–104.
Langer, L.F., Graybiel, A.M., 1989. Distinct nigrostriatal projection systems innervate striosomes and matrix in the primate striatum. Brain Res. 498, 344–350.
Li, L.B., Chen, N., Ramamoorthy, S., Chi, L., Cui, X.N., Wang, L.C., Reith, M.E., 2004. The role of N-glycosylation in function and surface trafficking of the human dopamine transporter. J. Biol. Chem. 279, 21012–21020.
Luo, Y., Roth, G.S., 2000. The roles of dopamine oxidative stress and dopamine receptor signaling in aging and age-related neurodegeneration. Antioxid Redox Sign 2, 449–460.
Marey-Semper, I., Gelman, M., Levi-Strauss, M., 1995. A selective toxicity toward cultured mesencephalic dopaminergic neurons is induced by the synergistic effects of energetic metabolism impairment and NMDA receptor activation. J. Neurosci. 15, 5912–5918.
Martres, M.P., Demeneix, B., Hanoun, N., Hamon, M., Giros, B., 1998. Up- and down-expression of the dopamine transporter by plasmid DNA transfer in the rat brain. Eur. J. Neurosci. 10, 3607–3616.
Melikian, H.E., Buckley, K.M., 1999. Membrane trafficking regulates the activity of the human dopamine transporter. J. Neurosci. 19, 7699–7710.
Nakatsukasa, K., Huyer, G., Michaelis, S., Brodsky, J.L., 2008. Dissecting the ER-associated degradation of a misfolded polytopic membrane protein. Cell 132, 101–112.
Przedborski, S., Jackson-Lewis, V., 1998. Mechanisms of MPTP toxicity. Mov. Disord. 13 (Suppl 1), 35–38.
Robinson, T.E., Mocsary, Z., Camp, D.M., Whishaw, I.Q., 1994. Time course of recovery of extracellular dopamine following partial damage to the nigrostriatal dopamine system. J. Neurosci. 14, 2687–2696.
Rodriguez, M., Abdala, P., Barroso-Chinea, P., Obeso, J., Gonzalez-Hernandez, T., 2001a. Motor behavioural changes after intracerebroventricular injection of 6-hydroxydopamine in the rat: an animal model of Parkinson's disease. Behav. Brain Res. 122, 79–92.
Rodriguez, M., Barroso-Chinea, P., Abdala, P., Obeso, J., Gonzalez-Hernandez, T., 2001b. Dopamine cell degeneration induced by intraventricular administration of 6-hydroxydopamine in the rat: similarities with cell loss in Parkinson's disease. Exp. Neurol. 169, 163–181.
Sandoval, V., Riddle, E.L., Ugarte, Y.V., Hanson, G.R., Fleckenstein, A.E., 2001. Methamphetamine-induced rapid and reversible changes in dopamine transporter function: an in vitro model. J. Neurosci. 21, 1413–1419.
Schmued, L.C., Albertson, C., Slikker Jr., W., 1997. Fluoro-Jade: a novel fluorochrome for the sensitive and reliable histochemical localization of neuronal degeneration. Brain Res. 751, 37–46.
Schmued, L.C., Hopkins, K.J., 2000. Fluoro-Jade: novel fluorochromes for detecting toxicant-induced neuronal degeneration. Toxicol. Pathol. 28, 91–99.
Schober, A., 2004. Classic toxin-induced animal models of Parkinson's disease: 6-OHDA and MPTP. Cell Tissue Res. 318, 215–224.
Stachowiak, M.K., Keller Jr., R.W., Stricker, E.M., Zigmond, M.J., 1987. Increased dopamine efflux from striatal slices during development and after nigrostriatal bundle damage. J. Neurosci. 7, 1648–1654.
Storch, A., Kaftan, A., Burkhardt, K., Schwarz, J., 2000. 6-Hydroxydopamine toxicity towards human SH-SY5Y dopaminergic neuroblastoma cells: independent of mitochondrial energy metabolism. J. Neural Transm. 107, 281–293.
Storch, A., Ludolph, A.C., Schwarz, J., 1999. HEK-293 cells expressing the human dopamine transporter are susceptible to low concentrations of 1-methyl-4-phenylpyridine (MPP+) via impairment of energy metabolism. Neurochem. Int. 35, 393–403.
Uhl, G.R., 2003. Dopamine transporter: basic science and human variation of a key molecule for dopaminergic function, locomotion, and parkinsonism. Mov. Disord. 18 (Suppl 7), S71–S80.
Uhl, G.R., Walther, D., Mash, D., Faucheux, B., Javoy-Agid, F., 1994. Dopamine transporter messenger RNA in Parkinson's disease and control substantia nigra neurons. Ann. Neurol. 35, 494–498.
Ungerstedt, U., 1971. Striatal dopamine release after amphetamine or nerve degeneration revealed a rotational behavior. Acta Physiol Scan. Suppl 367, 49–68.
Wang, Y.M., Gainetdinov, R.R., Fumagalli, F., Xu, F., Jones, S.R., Bock, C.B., Miller, G.W., Wightman, R.M., Caron, M.G., 1997. Knockout of the vesicular monoamine transporter 2 gene results in neonatal death and supersensitivity to cocaine and amphetamine. Neuron 19, 1285–1296.
West, M.J., 1999. Stereological methods for estimating the total number of neurons and synapses: issues of precision and bias. Trends Neurosci. 22, 51–61.
Williams, R.W., Rakic, P., 1988. Three-dimensional counting: an accurate and direct method to estimate numbers of cells in sectioned material. J. Comp. Neurol. 278, 344–352.

Woodgate, A., MacGibbon, G., Walton, M., Dragunow, M., 1999. The toxicity of 6-hydroxydopamine on PC12 and P19 cells. Brain Res. Mol. Brain Res. 69, 84–92.
Zhu, S.J., Kavanaugh, M.P., Sonders, M.S., Amara, S.G., Zahniser, N.R., 1997. Activation of protein kinase C inhibits uptake, currents and binding associated with the human dopamine transporter expressed in Xenopus oocytes. J. Pharmacol. Exp. Ther. 282, 1358–1365.
Zigmond, M.J., Abercrombie, E.D., Berger, T.W., Grace, A.A., Stricker, E.M., 1990. Compensations after lesions of central dopaminergic neurons: some clinical and basic implications. Trends Neurosci. 13, 290–296.
Zigmond, M.J., Stricker, E.M., 1973. Recovery of feeding and drinking by rats after intraventricular 6-hydroxydopamine or lateral hypothalamic lesions. Science 182, 717–720.